農業工程學報　第 63 卷第 2 期
中華民國 106 年 6 月出版

Journal of Taiwan Agricultural Engineering
Vol. 63, No. 2, June 2017

基於非接觸式紅外線溫度感測器單體之新型乾濕球濕度計設計

A Novel Design of Psychrometer Based on a Single-Packaged Contactless Infrared Thermometer

行政院農業委員會
臺南區農業改良場
助理研究員

李　健

Chien Li*

行政院農業委員會
臺南區農業改良場
副研究員

鍾 瑞 永

Jui-Yung Chung

摘　要

本文提出一個新型乾濕球濕度計的設計，透過一個非接觸式紅外線溫度感測器單體來量測懸掛於空氣流道中濕棉條的溫度來作為濕球溫度，並以感測器單體自身的封裝溫度感測來作為乾球溫度。其中空氣流道透過一個功率為 0.35 瓦的微型風扇來進行通風，此紅外線溫度感測器為出廠前已校正且具標準數位通訊介面的小型且低價感測模組。

在濕度快速演算部分，推導出飽和蒸氣壓五階多項式近似公式，使得演算能在一般低成本微控制器中快速執行。根據與 Goff-Gratch 公式的誤差分析，在 0°C~55°C 溫度範圍內以此方法得到相對濕度準確度能達到±0.02 以內，相較下一般常用的馬格努斯算式只能達到的±0.1 精度。

與基於兩根類比溫度感測棒的傳統乾濕球濕度計比較，本新型設計具有與棉球非接觸及感測器單體同時整合量測乾濕球兩者溫度的能力，帶來更精簡、可靠及易於數位整合的優點。

關鍵詞：乾濕球濕度計，濕球，相對溼度，飽和蒸汽壓，紅外線溫度。

ABSTRACT

A novel design of psychrometer is provided, where the air is pumped by a 0.35W mini-fan through a chamber with a hanged wet wick and a single-packaged contactless infrared thermometer aimed at the wick. The thermometer is a small size, low-cost, commercial off-the-shelf and comes factory-calibrated with a digital I^2C communication

*通訊作者，臺南區農業改良場作物環境課農業機械研究室助理研究員，71246 台南市新化區牧場 70 號，clee@mail.tndais.gov.tw

port, and it can measure both two temperatures of the package itself (dry bulb) and the wick surface (wet bulb).

For the fast computation of relative humidity (RH) in a generic microcontroller, a 5^{th}-order polynomial approximation equation for saturation vapor pressure is derived, which makes the calculation can be executed fast on the microcontroller. The error analysis with the Goff-Gratch equations shows that the computational accuracy for RH reading is within ±0.02 compared to ±0.1 of the Magnus approximate form at temperature range 0~55°C.

Compared to the conventional architecture of psychrometer based on two analog resistance temperature detectors (RTD), where one of them is soaked in the wet wick. The simple new design based on the contactless and combined temperature measurements has the advantages of compact, reliability, and digital integration.

Keywords: Psychrometer, Wet-Bulb, Relative Humidity, Saturation Vapor Pressure, Infrared Thermometer.

Introduction

Water can be found everywhere, and its vapor amount in the air, i.e. humidity, affects every aspect, e.g. living comfort for plant/animal, storage for matter, or factory for manufacturing food/semiconductor etc., a humidity sensor with reliability and accuracy is therefore very important to monitor or control the humidity of environments. The most common type of humidity sensor is on the basis of humidity-sensitive material (Chen *et al*., 2005; Rittersma, 2002), in which the material properties, i.e. capacitor, resistance or mechanical strain, will change with the humidity. Because of the required exposure to air, the sensing materials will age especially quickly in the hot and humid atmosphere (Nahar, 2000; Matsuguchi *et al*., 2000). The agricultural environments are even harsher for this type of sensor plus the chemical contaminants from fertilizers and pesticides clinging to sensing materials, so an accurate and robust method of measuring humidity is necessary in order to reduce the cost of refurbishment and recalibration.

The dry/wet-bulb psychrometer and chilled-mirror dew-point hygrometer (Wiederhold, 1997) compute the humidity based on temperatures, both methods not only provide an alternative way but also that the temperature sensors are immune to the aging or degradation because of the hermetic encapsulation. They, however, both need ventilation by a fan and regular maintenance, the psychrometer needs water refill and wick replacement for wet-bulb and the chilled mirror needs mirror cleaning. The chilled-mirror dew-point sensor (Jachowicz *et al*., 1993) which needs to precisely control the cooling power of mirror based on an optical feedback signal, however, is too expensive to be applicable in large extent to agriculture, although it attains the highest accuracy among other types due to the direct physical measurements of humidity.

Measuring humidity based on evaporative cooling of wet-bulb has a long history which can be traced back to the aspiration psychrometer (Assmann, 1892) that used a clockwork fan to draw air past the

Fig. 1 Common psychrometer for greenhouse made by Priva B.V. in Netherlands.

bulbs which were shielded from radiation by polished metal casings. With technological advancements, the original mercury thermometers were replaced by thermocouples (Powell, 1936) and it was also noticed that the wet-bulb depression T_{dry}-T_{wet} depends on the degree of ventilation, the diameter of the wire, the thickness and length of the water film covering the junction of the wet thermocouple, and the relative positions of the wet and dry thermocouples. Afterwards, a special design psychrometer was proposed (De Wit, 1953) which achieved sufficient ventilation by oscillating the dry/wet-bulb thermocouples, but this technique, perhaps some reasons, is up to now never taken into practical application. Except for the water refill, it had been proved that the psychrometer requires little maintenance and the dust accumulation barely affects the accuracy (Barber *et al*., 1989). On the contrary, it shows that dust contamination on chilled-mirror dew-point sensor can severe affect the reflected optical signal and make the calculated relative humidity apparently higher (Costello *et al*., 1991).

The Figure 1 shows the common psychrometer which has a fan with cross-section 80 × 80 mm^2 and 3.5W power rating, it's used in a greenhouse whose climate is controlled precisely for agricultural production. Although the old technology it has, psychrometers for now still play an indispensable role for durable humidity measurement in the harsh and critically-controlled agricultural environment, but it still has some drawbacks need to be improved as cited below. 1) First, in the viewpoint of digital integration, its two resistance temperature detectors (RTD), pt-100 or pt-1000, need the external reading circuit to convert the resistor of RTD to a digital signal. The standard of hermetic protections for its connecting wires and circuit board need to be strict in order to maintain the quality of analogous signal before converted, this results in higher module cost and size compared to a digital sensor probe. 2) Secondly, the RTD sensors are bulky in size, according to the former research findings (Zhao *et al*., 1992), the bigger wet-bulb size needs the air ventilation of higher volumetric flow rate, and this results in the use of a power-hungry bigger fan with a power rating more than 3W typically. 3) Thirdly, the RTD sensor of wet-bulb constantly contacts the wet wick, its surface will erode in the long term, and the accuracy of RTD is also affected. The RTDs for wet-bulb need replacements more frequently than those for dry-bulb in practice.

In this research, we propose the novel design of psychrometer based on one single-packaged infrared thermometer, which can measure both the dry/wet-bulb temperatures simultaneously. This new design improves or overcomes the aforementioned list of drawbacks, and its performance is also verified in the field test. In the following sections, the mechanical design and microcontroller-based reading circuit of the IR thermometer-based psychrometer are described. Then the derivation of a 5th-order polynomial approximation equation for saturation vapor pressure is shown, and its application to fast computation of relative humidity (RH) based on the dry/wet-bulb temperatures in a generic microcontroller is discussed. Finally, a field

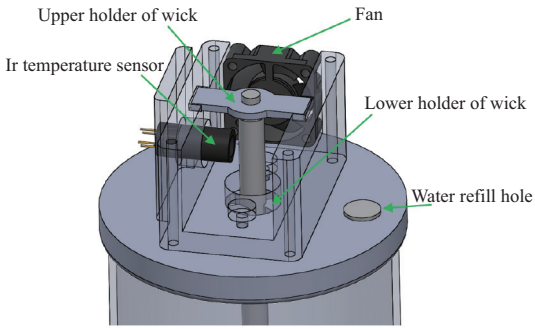

Fig. 2 Novel design of psychrometer with the upper cover removed, the fan has a 25 x 25 mm^2 cross-section area and a wind speed of 1.7 m/s with a 0.35W power rating. The size of IR thermometer is φ9 mm × 20 mm. The wet wick is fixed by the upper and lower holders.

test is conducted with the reference to two sensors having the accuracy of ±3% in RH.

Design

As the Figure 2 shows, with the upper cover removed, that the novel design of psychrometer is comprised of a reservoir for water, a chamber for air to flow through, a capillary wick (rope) which absorbs water from reservoir and hangs in the chamber, a mini-fan for ventilation, and finally an IR thermometer aimed at the wet wick. The mini-fan KD0502PFB3-8, manufactured by Sunon Co. Ltd., has a 25 × 25 mm^2 cross-section area and a wind speed of 1.7 m/s with a 0.35W power rating. The IR thermometer MLX90614 ESF-BCI, manufactured by Melexis N.V., is a small size (ϕ 9 mm × 20 mm), low-cost, commercial off-the-shelf and comes factory-calibrated with a digital I^2C communication port, and it can measure both two temperatures of the self-package (dry bulb) and the wick surface (wet bulb). The IR thermometer provides a 5-degree field-of-view for thermal radiation, and the thermometer needs to be close to the wet wick enough, depend on the field-of-view, to receive the thermal radiation exclusively from it. The IR thermometer can measure in the range of from –70 to +380°C for target temperature and that of from –40 to +125°C for package temperature of the device, it has the accuracy of 0.5°C over temperature range from 0 to +50°C and the measurement resolution of 0.02°C.

For the accurate measurement of IR thermometer, the emissivity of target surface must be taken into consideration, emissivity is a measure of the efficiency in which a surface emits thermal energy. It is defined as the fraction of energy being emitted relative to that emitted by a thermal black surface (a black body). A black body is a material that is a perfect emitter of heat energy and has an emissivity value of 1. For the band of wavelength 8~14 μm used by the IR thermometer, the emissivity of the wick, made of polypropylene, is 0.97, and that for water is 0.98. The reasonable emissivity can be chosen as 0.98 with regard to that the wick is wetted by water, the selected emissivity can be set up in the IR thermometer MLX90614 ESF-BCI through the digital I^2C communication port.

There are four wires connected to the IR thermometer, they are two power line (+3.3V、GND) and two line for I^2C port (SDA、SCL) respectively, the mini-fan is power by 5V source. The Figure 3 shows the microcontroller-based circuit board for interfacing the IR thermometer, text LCD display and a data logger. The adopted microcontroller is MSP430G2553 manufactured by Texas Instruments Inc., this microcontroller derives, through I^2C protocol, the dry/wet-bulb temperatures from the IR thermometer, and then calculate the relative humidity according to the 5th-order polynomial approximation equation for saturation vapor pressure, which will be mentioned later.

The popular two-wire I^2C protocol (SDA、SCL) provides the microcontroller with a convenient way to access multiple sensors of different types on the

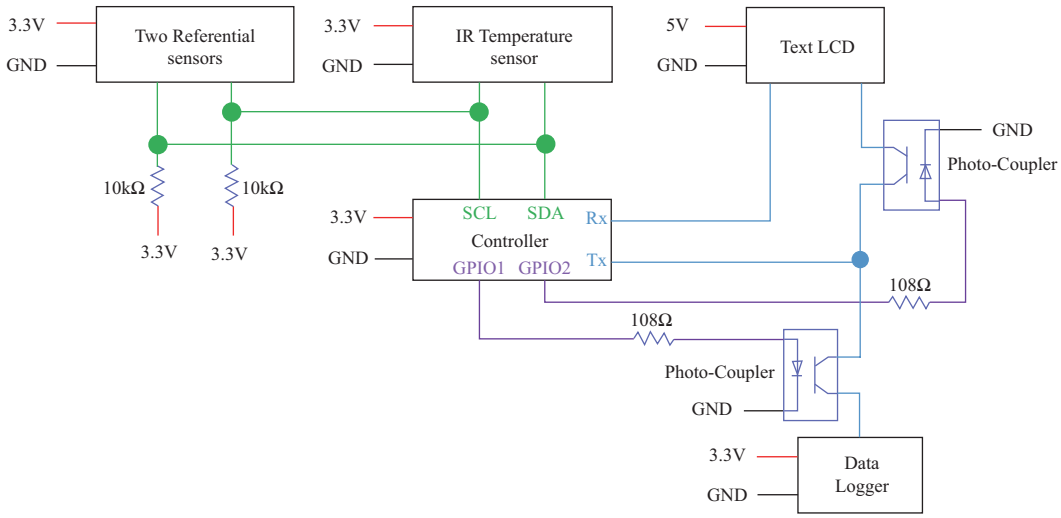

Fig. 3 Microcontroller-based circuit board made by ourselves for interfacing the IR thermometer, two referential sensors, a text LCD display, and a data logger. Either of the two photo-couplers is activated by the GPIO to switch the Tx port onto the Text LCD or data logger.

same rail as the IR thermometer. For a comparative test of the psychrometer with other commercial relative humidity sensors, two referential I^2C-based sensors can be arranged on the I^2C rail as shown in the Figure 3 to let the microcontroller access all of them on the same rail simultaneously.

All the measurement and calculations of data are processed in the microcontroller, then displayed on the text LCD in real-time and saved in the data logger every 30 seconds through sharing one switching UART transmit port (Tx), the port switching is conducted by the two photo-couplers controlled through the two GPIOs of microcontroller. Any generic microcontroller could easily provide the flexible bridge to connect the psychrometer with other digital things, thanks the standard I^2C and UART protocols.

Computation Equations

Humidity or moisture content can be expressed in a number of ways, the most common one is the relative humidity (RH), which is

$$\mathrm{RH} = e / e_s \qquad \text{..... (1)}$$

where e is the actual vapor pressure, it is the partial pressure of water vapor in the air, and e_s is the saturation vapor pressure, the highest partial pressure the water vapor can achieve at specified air temperature.

When the atmosphere pressure is fixed, the saturation vapor pressure e_s is the function of temperature T alone. The function expression for $e_s(T)$ is the important basis for calculation of RH based on the dry and wet-bulb temperature T_{dry} and T_{wet}. The relationship (Sargent, 1980) between e, T_{dry} and T_{wet} can be expressed as

$$e_s|_{T=T_{wet}} - e = \alpha P_{atm}(T_{dry} - T_{wet}) \qquad \text{..... (2)}$$

where α is the psychrometric coefficient related to the ventilation condition of wet-bulb, α can be saw as a constant 6.53×10^{-4} 1/°C with the sufficient ventilation. P_{atm} is the atmosphere pressure, its value is 1013.25 *mbar* at sea level.

The vapor pressure at the wet-bulb surface is

seen as saturated and can be expressed as $e_s|_{T=T_{wet}}$. The left term of equation (2), the vapor pressure difference, is the driving potential for the evaporation of wet-bulb water to air, and the right term, the temperature difference, is that potential for heat transfer from air to the wet-bulb. Equation (2), therefore, describes the balance of evaporative water mass and latent heat (Simões-Moreira, 1999). Over the past hundred years, the mathematical relationship between e_s and temperature T has been discussed extensively (Gibbins, 1990), among the myriad of equations the Goff-Gratch equation (Goff & Gratch, 1945) is recommended by World Meteorological Organization (WMO, 2012) as the standard reference for temperature range from −100°C~100°C, it has the form as bellow

$$\log\left(\frac{e_s}{P_{atm}}\right) = -7.90298(T'-1) + 5.02808\log T' - 1.3816\times10^{-7}\left[10^{11.344\left(1-\frac{1}{T'}\right)}-1\right] + 8.1328\times10^{-3}\left[10^{-3.49149(T'-1)}-1\right] \quad (3)$$

where

$$T' = 373.16/(273.16+T)$$

and

$$P_{atm} = 1013.246 mbar$$

Because of the inconvenient application of the complicated Goff-Gratch equation, the World Meteorological Organization suggests an approximate equation of Magnus form for a temperature range of –45°C~60°C (Magnus, 1844; WMO, 2012). The approximate Magnus equation is shown as bellow

$$\overline{e}_s(T) = 6.112\exp\left(\frac{17.62T}{243.12+T}\right) \quad \text{.....(4)}$$

For the computation in microcontroller, the exponential term in equation needs to be decomposed into power series as bellow

$$\exp(x) = \sum_{n=0}^{\infty}\frac{x^n}{n!} = 1 + x + \frac{x^2}{2!} + \frac{x^3}{3!} + \cdots \text{ ..... (5)}$$

For the sufficient accuracy, the number n of equation (5) needs to be large enough, this computation is hardly achieved in a generic microcontroller. In order to solve that, some research (Lowe, 1977) proposed the adoption a six-order polynomial approximate equation for saturation vapor pressure e_s, with intended use at temperature range –50°C~50°C. Later another research (Flatau *et al*., 1992) further used an eight-order polynomial one to calculate e_s with the wider temperature range of –85°C~70°C.

Calculating e_s through polynomial approximate equation is efficient and easy to realize in digital device, the methods for interpolating polynomial equation have the very useful applications. In general, the polynomial approximate equations can be derived through the Lagrange interpolation by providing the setting points, it will need n + 1 setting points for an n^{th}-order polynomial equation. In this article a fifth-order polynomial is used to approximate e_s for range of –5°C~55°C as bellow

$$\overline{e}_s(T) = a_0 + a_1T + a_2T^2 + a_3T^3 + a_4T^4 + a_5T^5 \quad . (6)$$

where a_0, a_1, … a_5 is the coefficients which can be derived from the inverse of Vandermonde matrix as bellow

$$\begin{bmatrix} a_0 \\ a_1 \\ \vdots \\ a_5 \end{bmatrix} = \begin{bmatrix} 1 & \cdots & T_0^4 & T_0^5 \\ 1 & \cdots & T_1^4 & T_1^5 \\ \vdots & & \vdots & \vdots \\ 1 & \cdots & T_5^4 & T_5^5 \end{bmatrix}^{-1} \times \begin{bmatrix} e_s(T_0) \\ e_s(T_1) \\ \vdots \\ e_s(T_5) \end{bmatrix} \text{ ..... (7)}$$

where T_0, T_1, … T_5 are temperatures of the six setting point for Lagrange interpolation, and $e_s(T_0)$, $e_s(T_1)$, … $e_s(T_5)$ is the saturation vapor pressures

based on the Goff-Gratch equation (3).

The temperatures for six setting points is selected as −5°C、7°C、19°C、31°C、43°C、55°C with equal spans, and through equation (3) and (7) a fifth-order polynomial to approximate e_s will be derived as

$$\begin{aligned}\overline{e}_s(T) &= 6.109 + 0.444T + 1.424\times10^{-2}T^2 + 2.715\times10^{-4}T^3 + 2.697\times10^{-6}T^4 + 2.785\times10^{-8}T^5 \\ &= \Big(\big(\big((0.02785T + 2.697)T + 271.5\big)T + 14240\big)T + 444000\Big)T\times10^{-6} + 6.109\end{aligned} \quad \text{..... (8)}$$

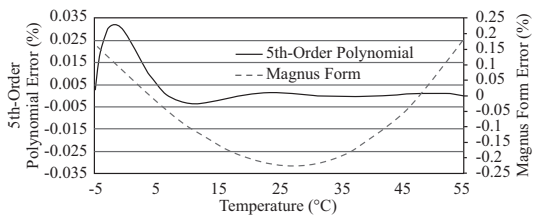

Fig. 4 Saturation vapor pressure error percentage for 5th-order polynomial and Magnus form with Goff-Gratch equation.

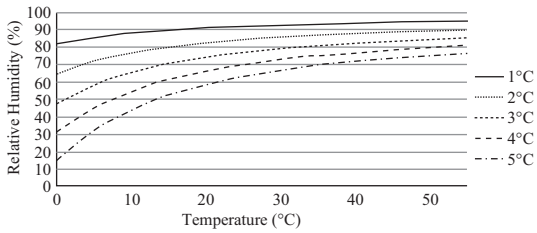

Fig. 5 Relative humidity based on Goff-Gratch equation with $T_{dry} - T_{wet}$ from 1°C to 5°C.

where the factored form for the polynomial could be executed more efficiently in programming code

With the Goff-Gratch equation as a gold standard, the error percentage for approximate equation of Magnus (4) or polynomial (6) can be written as

$$error(\%) = \frac{\overline{e}_s(T) - e_s(T)}{e_s(T)} \times 100\% \quad \text{.....(9)}$$

where $e_s(T)$ is provided by Goff-Gratch equation (3), and $\bar{e}_s(T)$ is given by approximate equation (4) or (8).

Figure 4 shows, on the whole, that the error percentage for $e_s(T)$ of fifth-order polynomial equation (6) is, on average, 30 times less than that of Magnus equation (4) over −5°C~55°C temperature range. It prove that for a modest temperature range the fifth-order approximate polynomial can possess both accuracy and computational efficiency than the approximation of Magnus form.

The relative humidity RH based on T_{dry} and T_{wet} can be derived by substituting equation (2) into (1) as

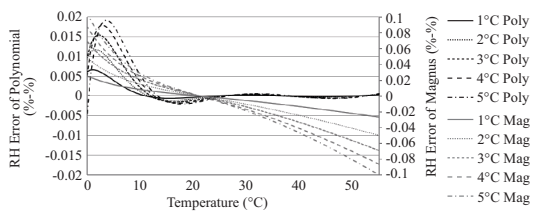

Fig. 6 Relative humidity differences on different $T_{dry} - T_{wet}$ for 5th-order polynomial and Magnus form.

$$RH = \frac{e_s\,|_{T=T_{wet}} - \alpha P_{atm}(T_{dry} - T_{wet})}{e_s\,|_{T=T_{dry}}} \quad \text{..... (10)}$$

The RH values calculated based on the Goff-Gratch equation, for different wet-bulb depression $T_{dry} - T_{wet}$ are shown on the Figure 5, it is noted that the RH values are more exclusively correlated to wet-bulb depression when the air temperature is higher. Figure 6 shows the RH differences between the RH values calculated by approximate equation and those by Goff-Gratch equation for the 5th-order polynomial and Magnus

form respectively. The RH differences are higher for both with a higher wet-bulb depression, and those for 5th-order polynomial suddenly rise when the air temperature is bellow 10°C. Most important of all, the RH differences for polynomial are within ±0.02 compared to ±0.1 of the Magnus form at temperature range 0~55°C

Results & Discussion

A field test of the novel design of psychrometer was executed for 30 days, which is also accompanied by two referential sensors aside. The environment of the test is a warehouse, the two referential sensors HTU21D with board size 15 × 15 mm^2, made by Measurement Specialties Inc., have an accuracy of ±3% for relative humidity and their measurements are digitally transmitted to a data logger. The reason to use two referential sensors is to make sure that both of them function accordingly without any great deviation. Both the psychrometer and two referential sensors record the atmospheric data simultaneously and synchronically, and the sampling interval is 30 seconds. The comparison test continuously runs without any intervention, its objective is to verify the feasibility of psychrometer design in practice.

The natural variations of T_{dry}, T_{wet}, and calculated RH for field test are shown in the Figure 7, this one-month long test is intended to comprise all kinds of transient responses and humidity states as could as possible. The differences between the calculated RH of psychrometer and two referential sensors are plotted as two locus in the Figure 8, the two locus of RH difference are roughly within +2 to −1 except for some minor excursions which are caused by the more sluggish responses of psychrometer. The greatest excursion occurred at day 18.08 to day 18.1 in the Figure 7, and that segment is excerpted to the Figure 9, where the sudden rise of RH from 52% to 60% within 5 minutes caused the maximum difference approaching −4 in the Figure 8. The low response of the psychrometer stems from that it takes the

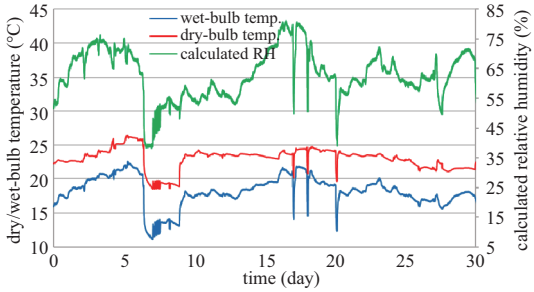

Fig. 7 Variations of T_{dry}, T_{wet}, and calculated RH for field test.

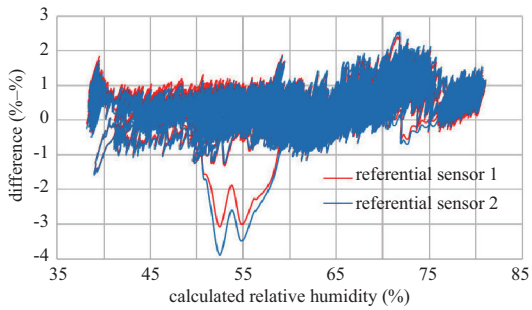

Fig. 8 Differences between the calculated RH of psychrometer and two referential sensors are plotted as two locus.

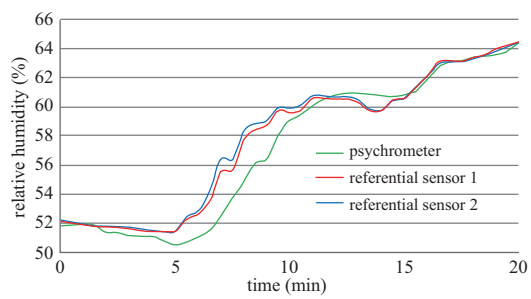

Fig. 9 Sudden rise of RH from 52% to 60% within 5 minutes cause the greatest excursion in Figure 9.

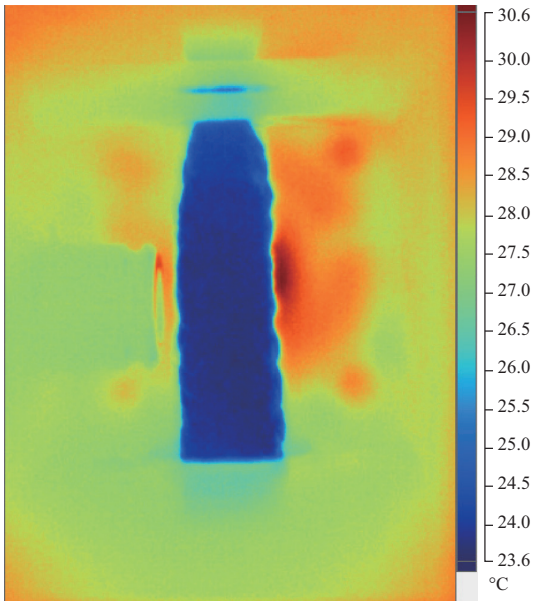

Fig. 10 Thermal image of air channel inside psychrometer

time to reach thermal equilibrium for the wet wick and sensor package, this shortcoming could be further improved by developing a smaller infrared thermometer, which is also compatible to a smaller wick, in the future.

The Figure 10 shows the thermal image of air channel inside psychrometer, the wet wick is uniformly cooled by evaporative water, and the hot motor of fan is shown in the background. The infrared thermometer is situated to the left side of wick as the Figure 2 depicts, the artifact hot surface on the frontend of thermometer is caused by the reflection of thermal radiation from background.

Conclusions

In the novel design of psychrometer, the air is pumped by a mini-fan through a chamber with a hanged wet wick and a single-packaged contactless infrared thermometer aimed at the wick. The infrared thermometer is a small size (ϕ 9 mm × 20 mm), commercial off-the-shelf and comes factory-calibrated with a digital I^2C communication port, it measures both two temperatures of the package itself (dry bulb) and the wick surface (wet bulb).

The Table 1 show a benchmark of different technology for measuring humidity in air, compared to the conventional architecture of psychrometer based on two analog resistance temperature detectors (RTD), where one of them is soaked in the wet wick. This simple new design based on the contactless and integrative temperature measurements has the advantages of compact, reliable, cost-effective and easy digital integration. In addition, the mini-fan (25 × 25 × 10 mm^3) has a 0.35W power rating, which is ten times less than a generic fan (80 × 80 × 25 mm^3) used in conventional psychrometer. It also provides an alternative choice to the most common RH sensors based on sensing material when the environmental condition is harsh and they suffer the problem of drift. According to the temperature accuracy of the IR sensor used in this research and the datasheet of commercial Psychrometer products (e.g. the psychrometer SK-5RAD-SP made by Sato Keiryoki Mfg. in Japan), the accuracy of RH measurement can be reasonably estimated to be about ±2%

A 5^{th}-order polynomial approximation equation for saturation vapor pressure is derived for the fast computation of relative humidity (RH) in a generic microcontroller, which makes the calculation can be executed fast on the microcontroller. The error analysis with the gold-standard Goff-Gratch equations shows that the computational accuracy for RH reading is within ±0.02 compared to ±0.1 of the Magnus approximate form at temperature range 0~55°C. For a moderate temperature range, the speed and accuracy of 5^{th}-order polynomial are both better than the common Magnus equation.

A field test for comparison was executed for 30 days, which is also accompanied by two referential sensors with an accuracy of ±3% for RH

Table 1 A benchmark of different technology for measuring humidity in air

	Contactless IR Psychrometer	Conventional Two RTD Psychrometer	RH Sensor based on sensing material
Accuracy (0~50℃)	In this research ±0.5°C (~±2% RH)	• For RTD of class A： ±0.25°C (~±1% RH) • For RTD of class B： ±0.55°C (~±2% RH) According to IEC 751 standard	±2% or ±3% depend on manufacturer's specification
Possible Durability Problem	Probably no problem, but still need a long-term test of several years to verify	• Degraded hermetic protection for RTD converting circuit board • Surface erosion on the casing of RTD sensor for wet-bulb	The chemical contamination, high humid and high temperature all could cause severe drift on sensors
Hardware Complexity (w/o controller)	• Small single-package sensor (ϕ 9 mm × 20 mm) • Mini-fan (25 × 25 mm^2) • Compact casing	• Two long RTD temp. probe (ϕ 6 mm × 80 mm typically) • bigger fan (80 × 80 mm^2) • Two converting circuits for RTD • huge casing for accommodation	Small SMT sensor bonded on circuit board (20 × 15 mm^2 typically)
Maintenance	• Water refill • Wick wash • Cleaning of IR lens	• Water refill • Wick wash	None
Cost	~NT$1000	~NT$3000	~NT$300
Digital Integration	Convenient (I^2C)	Need additional processing by hardware	Convenient (I^2C)
Power Consumption	~0.36W (mostly by fan)	~3.5W (mostly by fan)	~0.0027W

aside, the environment of the test is an office room without any air conditioner. RH difference between psychrometer and two referential sensors are roughly within from +2 to −1 except for some minor excursions which are caused by the more sluggish responses of a psychrometer. The greatest excursion is attributed to the sudden rise of RH from 52% to 60% within 5 minutes which caused the maximum difference approaching −4

This new design of psychrometer based on infrared thermal sensing technique possesses the potential for miniaturization and reducing electric power for ventilation in the future. With the advance of MEMs and Microelectronics technology, there are already several types of Infrared thermal sensor chips, which have the Wafer-Level-Chip-Scale-Package WLCSP (1.6 × 1.6 × 0.625 mm^3), made by Texas Instruments Inc.

Acknowledgment

The authors would like to thank the financial support by Council of Agriculture in Taiwan with the grant number：105AS-8.3.2-NS-N2.

References

1. Assmann, R., "Aspiration psychrometer", Zeitschrift für Instrumentenkunde, 12:1-12, 1892.
2. Barber, E. M., and Gu, D., "Performance of an aspirated psychrometer and three hygrometers in livestock barns", Applied Engineering in Agriculture, 5(4):595-600, 1989.
3. Chen, Zhi, and Lu, Chi, "Humidity sensors: a review of materials and mechanisms", Sensor Letters, 3:274-295, 2005.

4. Costello, T. A., Berry, I. L., and Benz, R. C., “A fan-actuated mechanism for controlled exposure of a psychrometer wet buld sensor to a dusty environment”, Applied engineering in agriculture, 7(4):473-477, 1991.
5. De Wit, C. T., “An oscillating psychrometer for micro-meteorological purposes”, Applied Scientific Research, Section A, 4(2):120-126, 1953.
6. Flatau, Piotr J., Walko, Robert L., and Cotton, William R., “Polynomial Fits to Saturation Vapor Pressure”, Journal of Applied Meteorology, 31:1507-1513, 1992.
7. Goff, J. A., and Gratch, S., “Thermodynamic properties of moist air”, Amer. Soc. Heat. Vent. Eng. Trans., 51:125-157, 1945.
8. Gibbins, C. J., “A survey and comparison of relationships for the determination of the saturation vapour pressure over plane surfaces of pure water and of pure ice”, Ann. Geophys., 8:859-885, 1990.
9. Jachowicz, R. S., and Makulski, W. J., “Optimal measurement procedures for a dew point hygrometer system”, Instrumentation and Measurement, IEEE Transactions on, 42(4): 828-833, 1993.
10. Lowe, Paul R., “An Approximating Polynomial for the Computation of Saturation Vapor Pressure”, Journal of Applied Meteorology, 16: 100-103, 1977.
11. Magnus, G., “Versuche uber die Spannkrafte des Wasserdampfs”, Ann. Phys. Chem., 61: 225-247, 1844.
12. Matsuguchi, M., Hirota, E., Kuroiwa, T., Obara, S., Ogura, T., and Sakai, Y., “Drift Phenomenon of Capacitive-Type Relative Humidity Sensors in a Hot and Humid Atmosphere”, Journal of the Electrochemical Society, 147(7): 2796-2799, 2000.
13. Nahar, R. K., “Study of the performance degradation of thin film aluminum oxide sensor at high humidity”, Sensors and Actuators B: Chemical, 63(1):49-54, 2000.
14. Powell, R. W., “The use of thermocouples for psychrometric purposes”, Proceedings of the Physical Society, 48(3):406, 1936.
15. Rittersma, Z. M., “Recent achievements in miniaturised humidity sensors—a review of transduction techniques”, Sensors and Actuators A: Physical, 96(2):196-210, 2002.
16. Sargent, G. P., “Computation of vapour pressure, dew-point and relative humidity from dry- and wet-bulb temperatures”, Meteor. Mag., 109:238-246, 1980.
17. Simões-Moreira, J. R., “A thermodynamic formulation of the psychrometer constant”, Measurement Science and Technology, 10(4):302, 1999.
18. Wiederhold, Pieter R., Water vapor measurement: methods and instrumentation, CRC Press, Boca Raton, Florida, 1997.
19. World Meteorological Organization, Technical Regulations (WMO-No. 49), Volume I: General Meteorological Standards and Recommended Practices, WMO, Geneva, Switzerland, 2012.
20. Zhao, Y., Jiang, B., and Fang, H., “Experimental study of the effects of wind speed, radiation, and wet bulb diameter on wet bulb temperature”, Experimental thermal and fluid science, 5(6):790-794, 1992.

收稿日期：民國 105 年 7 月 26 日
修正日期：民國 105 年 9 月 10 日
接受日期：民國 105 年 10 月 4 日